Electronic Supplementary Material (ESI) for Journal of Materials Chemistry A.

Supporting Information

Molecular-level electrochemical doping for fine discrimination of volatile organic compounds in organic chemiresistors

Sooncheol Kwon[a*†], Yusin Pak[b†], Bongseong Kim[d], Byoungwook Park[c], Jehan Kim[e], Geunjin Kim[d], Yong-Ryun Jo[c], Saurav Limbu[f], Katherine Stewart[f], Hyeonghun Kim[c], Bong-Joong Kim[c], Soo-Young Jang[a], Hongkyu Kang[a], Jung-Wook Min[g], Ji-Seon Kim[f*], Gun Young Jung[c*] and Kwanghee Leea[c*]

[a] Research Institute for Solar and Sustainable Energies (RISE), Gwangju Institute of Science and Technology (GIST), Gwangju 500-712, Republic of Korea. E-mail: kwansc@gist.ac.kr
[b] Sensor System Research Center (SSRC), Korea Institute of Science and Technology (KIST), Seoul 02792, Republic of Korea.
[c] School of Materials Science and Engineering (SMSE), Gwangju Institute of Science and Technology (GIST), Gwangju 500-712, Republic of Korea. E-mail: klee@gist.ac.kr
[d] Heeger Center for Advanced Materials (HCAM), Gwangju Institute of Science and Technology (GIST), Gwangju 500-712, Republic of Korea.
[e] Pohang Accelerator Laboratory, Pohang University of Science and Technology, Pohang 37673, Republic of Korea.
[f] Department of Physics and Centre for Plastic Electronics, Imperial College London, London, SW7 2AZ, United Kingdom.
[g] Physical Sciences and Engineering Division, King Abdullah University of Science and Technology (KAUST), Thuwal, Kingdom of Saudi Arabia

*Correspondence to: kwansc@gist.ac.kr; ji-seon.kim@imperial.ac.uk; gyjung@gist.ac.kr; klee@gist.ac.kr

†S. K. and Y. P. contributed equally to this work.

Table S1. Summary of recent publications on chemiresistors based on inorganic or hybrid materials for detecting acetone and toluene and comparison with the sensing capability of the TT:SIL TOCs developed in this work.

Materials	Operation Temp. (^{o}C)	Target VOC	LOD (ppm)	Responsivity (%)	Response /Recovery (s)	Reference
PtPd-WO_3 NF (Inorganic)	300	Acetone	0.001	9750 (at 1 ppm)	<4.2 / <204	31
Pt@In_2O_3 NF (Inorganic)	320	Acetone	0.01	623 (at 1 ppm)	11 / 13	32
V_2O_5 nanoneedle (Inorganic)	R.T.	Acetone	1.7	137 (at 140 ppm)	70 / -	33
Pd-@ZnO-WO_3 NF (Inorganic)	350	Toluene	< 0.1	2222 (at 1 ppm)	20 / -	34
Poly(DTCPA-co-BHTBT) – carbon black (Hybrid)	R.T.	Toluene	15	0.5 (at 150 ppm)	35 /84	35
TiO_2-decorated 3D Graphene-CNT (Hybrid)	R.T.	Toluene	50	4 (at 100 ppm)	6/7	36
TT:SIL (Organic)	R.T.	Acetone	0.34	2.1 (at 20 ppm)	180/180	This work
		Toluene	0.41	1.7 (at 20 ppm)	180/180	

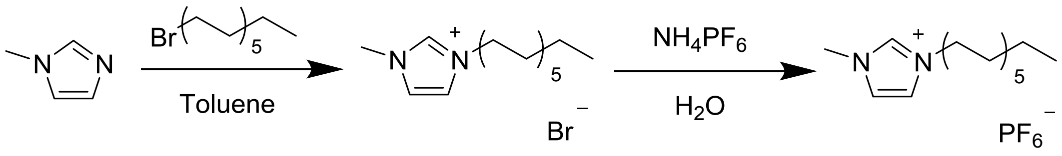

C_1C_{12}IMBr **C_1C_{12}IMPF$_6$**

Fig. S1. Synthetic scheme for $[C_1C_{12}IM]^+[Br]^-$ and $[C_1C_{12}IM]^+[PF_6]^-$.

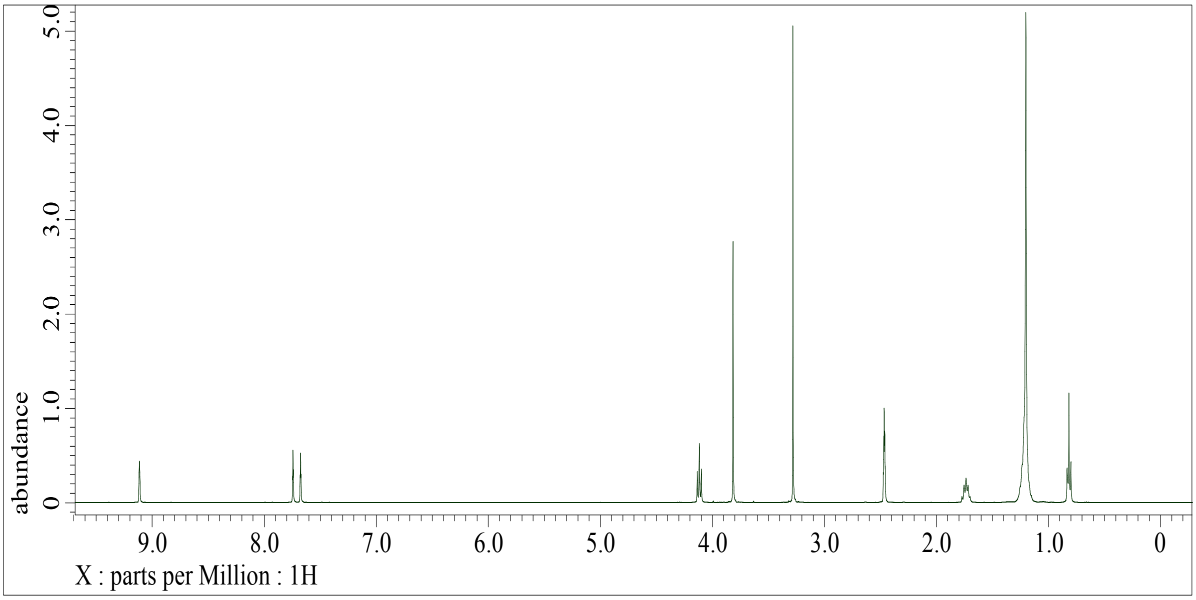

Fig. S2. Nuclear magnetic resonance (NMR) data of $[C_1C_{12}IM]^+[Br]^-$.

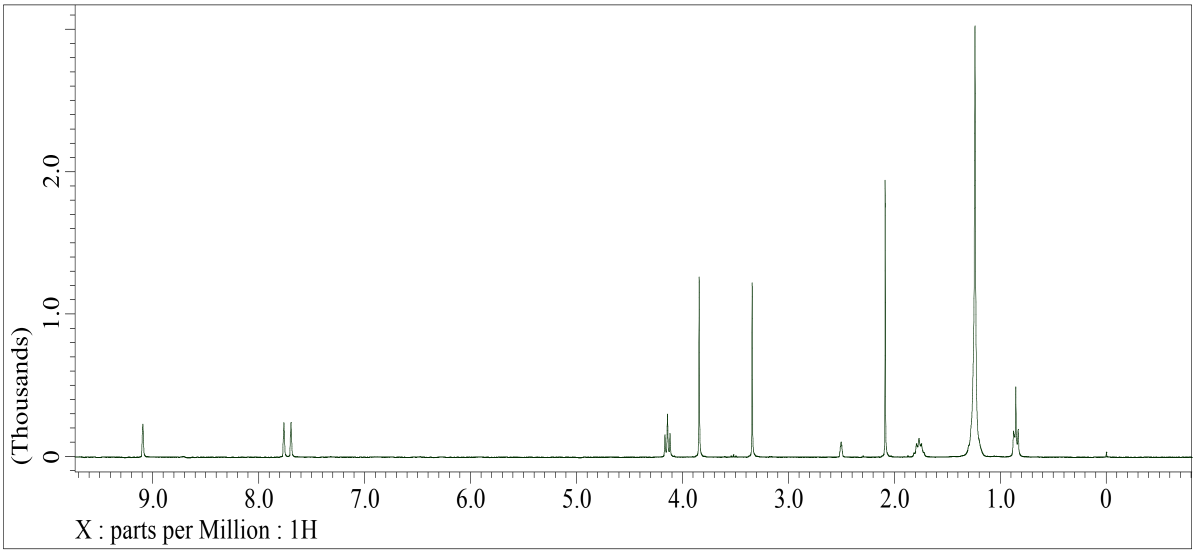

Fig. S3. NMR data of $[C_1C_{12}IM]^+[PF6]^-$.

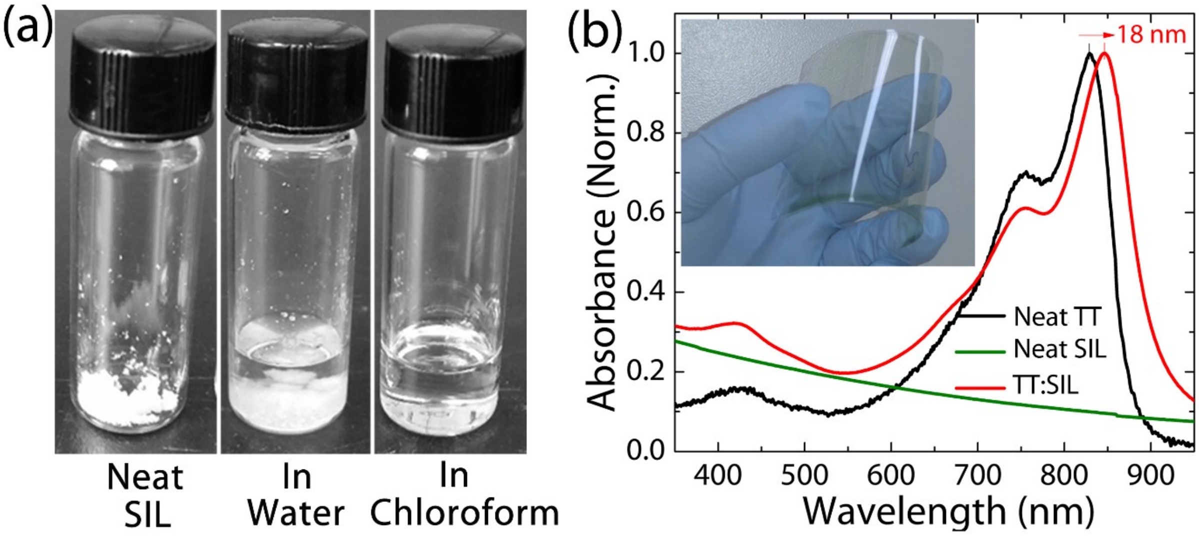

Fig. S4. **(a)** Comparison of the solubilities of the SIL in water (polar solvent) and chloroform (nonpolar solvent). (**b**) Normalized absorption spectra of as-cast neat TT, neat SIL and TT:SIL blend (1:5 w/w) films. The inset is a photograph of a TT:SIL film on a flexible PEN substrate.

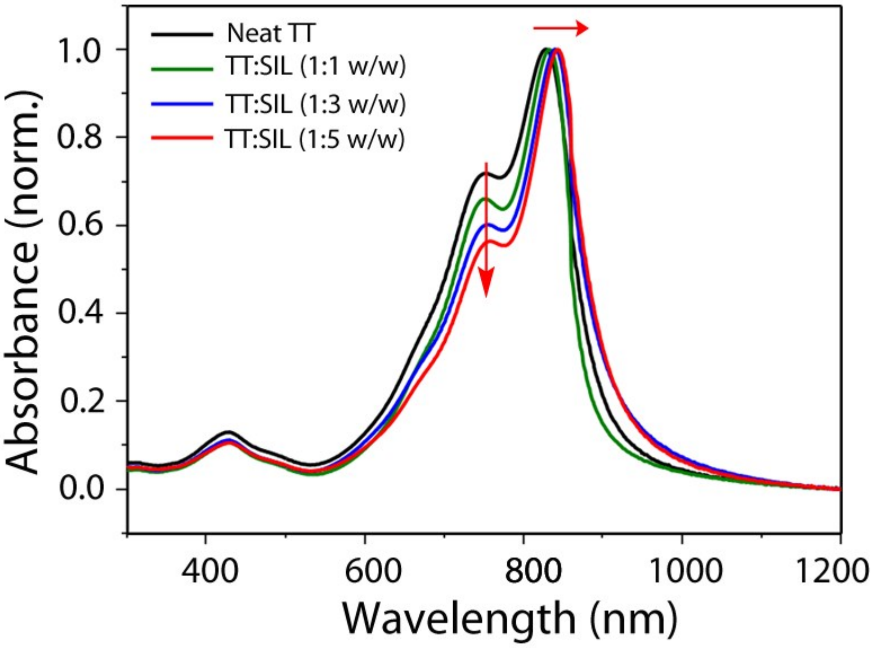

Figure S5. The optical absorption spectra of neat TT and TT:SIL (1:1, 1:3 and 1:5 w/w) thin films were obtained using a UV-Vis spectrometer. The neat TT polymer exhibited typical features of a vibronically structured 0-0 transition, with an onset at 920 nm, whereas the TT:SIL blend films exhibited absorption spectra that were similar to that of the pristine TT polymer, except for the gradual redshift (up to ~18 nm) in the maximum absorption peak of the blended films at 830 nm as the blend ratio increased. In particular, the increase in the relative ratio of the 0-0:0-1 transition of the TT:SIL film vs. the neat TT polymer film implies that the SIL enhances the intermolecular interactions of the TT polymer chains.

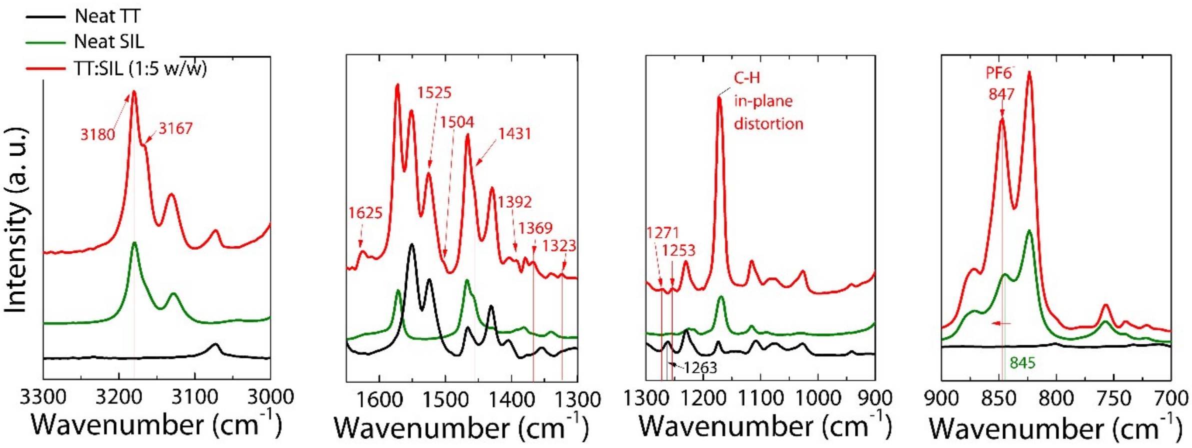

Fig. S6. The two major peaks between 3100 and 3200 cm^{-1} were assigned to the aromatic C–H stretching vibrations in the imidazolium cation, while the peaks between 800 and 900 cm^{-1} originated from the $[PF_6]^-$ anion of the SIL. When the SIL is mixed with the TT polymer, the original peaks from the cations and anions of the SIL become sharper, and the peaks at 1572 cm^{-1} and 845 cm^{-1}, which represent the C=N$^+$ vibration mode of the imidazolium cation and the FP-F asymmetric stretching mode of the $[PF_6]^-$ anion, respectively, are blueshifted. This result indicates that the ionic interactions between the cations and anions of the SIL became weaker after blending with TT. In addition, compared with those of the other SIL peaks, the intensities of the peaks at 3167 cm^{-1} and 847 cm^{-1} increased after mixing with the TT polymer, which suggests that a change in the molecular interactions between the ions of the SIL occurs upon the addition of the TT polymer. Several new peaks (e.g., peaks at 1625, 1369, 1323, 1271, and 1253 cm^{-1}) appeared in the spectra of the TT:SIL blend, and the peaks at 1354 and 1263 cm^{-1} disappeared from the spectrum. In particular, the peak at 1263 cm^{-1}, which is attributed to the aromatic amine group of the DPP units in the TT polymer, could be split into two new peaks at 1271 cm^{-1} and 1253 cm^{-1} due to perturbation by neighboring molecules, which, in this case, were the ions of the SIL. This result is in accordance with the strong intermolecular interactions indicated by the change in the absorption spectra after the addition of the SIL to the TT polymer.

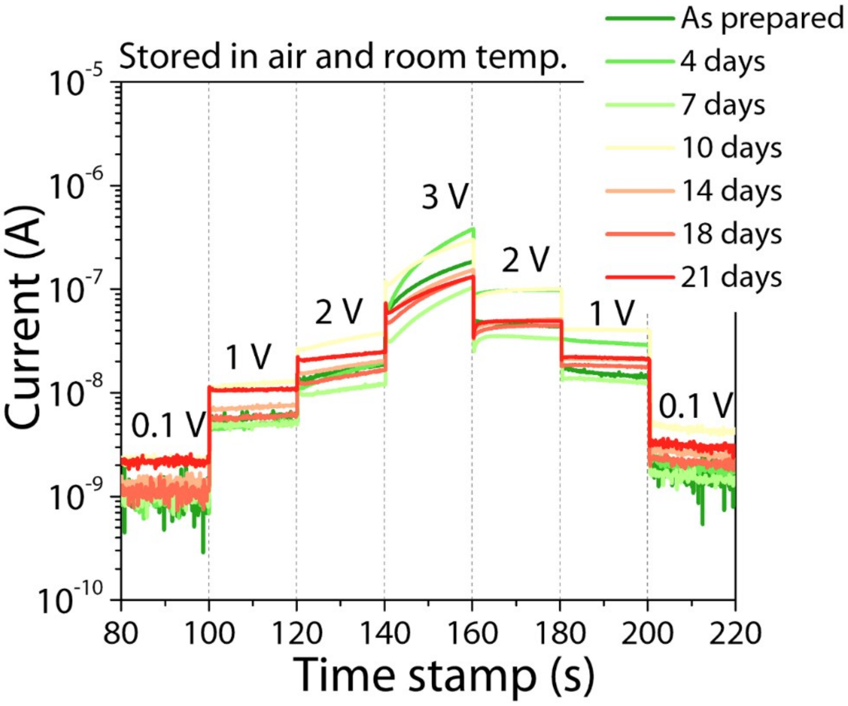

Fig. S7. Stability test for TT:SIL (1:5 w/w) TOCs (L = 20 μm, W = 3000 μm) that are stored in air and room temperature conditions for 3 weeks (21 days); the V_{ds} values range from 0.1 V to 3 V.

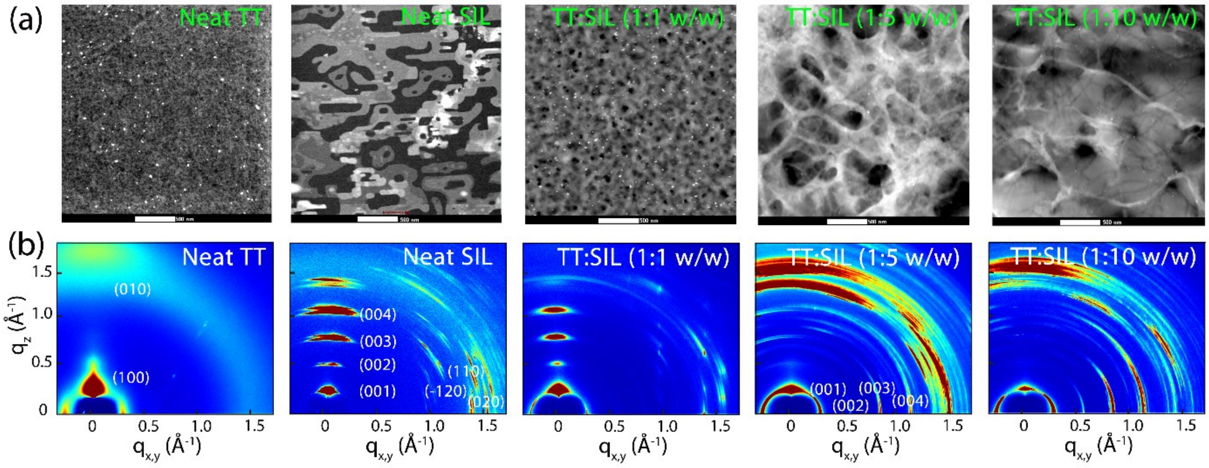

Fig. S8. (a) HAADF-STEM images of the neat TT, neat SIL and TT:SIL films with different ratios (i.e., TT:SIL = 1:1, 1:5, and 1:10 weight/weight). The scale bar is 500 nm. The formation of fibrous structures in the TT:SIL film becomes increasingly evident with increasing SIL concentrations. **(b)** The corresponding 2-D GIWAXS images of the neat TT, neat SIL and TT:SIL films.

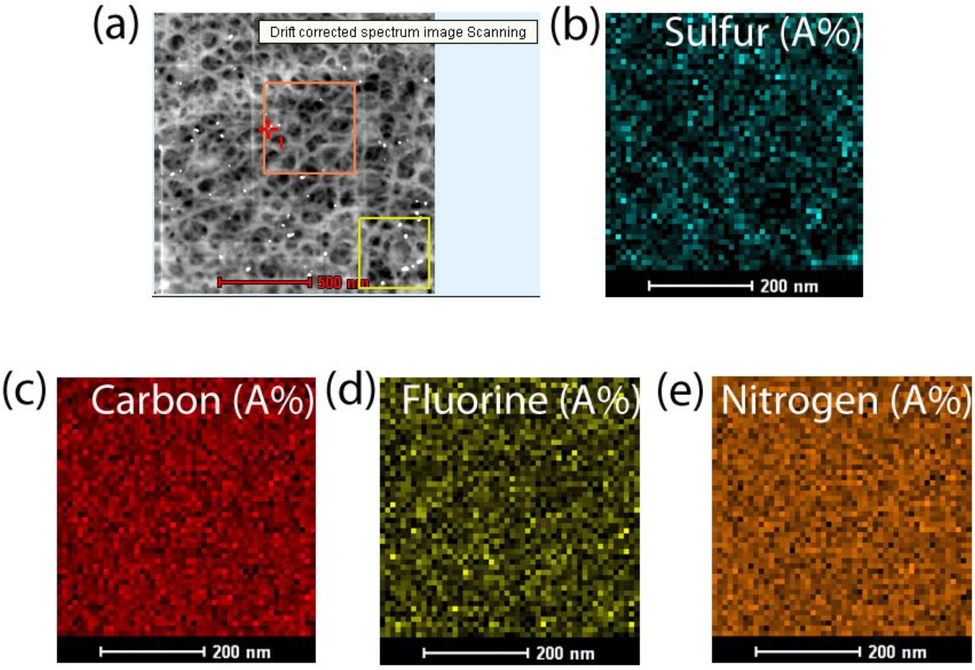

Fig. S9. (a) HAADF-STEM images of TT:SIL (1:5 w/w) film. Orange and yellow squares indicate the 2-dimentional scan area and position reference, respectively, for elemental mapping. Results of the elemental mapping (Atomic %) on the corresponding film for **(b)** sulfur, **(c)** carbon, **(d)** fluorine and **(e)** nitrogen using energy-dispersive X-ray spectroscopy (EDXS) technique. Sulfur can be thought to be a representative element in the TT polymer, while fluorine can be thought to be a representative element in SIL.

Determining crystalline structure and structural parameters of solid-state ionic liquid (SIL) based on GIWAXS data

We define the crystal structure of SIL through 3 steps as follows;

1) **Step 1 : We define relations among angles and axes for SIL.**

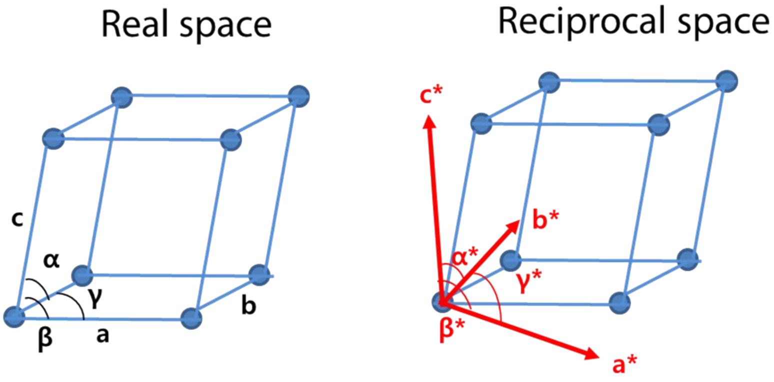

$$a = 2\pi \frac{b^* \times c^*}{a^* \cdot (b^* \times c^*)},\quad b = 2\pi \frac{c^* \times a^*}{a^* \cdot (b^* \times c^*)},\quad c = 2\pi \frac{a^* \times b^*}{a^* \cdot (b^* \times c^*)}$$ where

$a^* = 2\pi / d_{100} = q_{100}$, $b^* = 2\pi / d_{010} = q_{010}$, $c^* = 2\pi / d_{001} = q_{001}$.

Also, we define the angles between the axes as follows;

$$\cos(\alpha) = \frac{\cos(\beta^*)\cos(\gamma^*) - \cos(\alpha^*)}{\sin(\beta^*) \cdot \sin(\gamma^*)},\quad \cos(\beta) = \frac{\cos(\gamma^*)\cos(\alpha^*) - \cos(\beta^*)}{\sin(\gamma^*) \cdot \sin(\alpha^*)},$$

$$\cos(\gamma) = \frac{\cos(\alpha^*)\cos(\beta^*) - \cos(\gamma^*)}{\sin(\alpha^*) \cdot \sin(\beta^*)}$$

where

$$\cos(\alpha^*) = \frac{(q_{011}{}^2 - q_{010}{}^2 - q_{001}{}^2)}{2 \cdot q_{010} \cdot q_{001}},\quad \cos(\beta^*) = \frac{(q_{101}{}^2 - q_{100}{}^2 - q_{001}{}^2)}{2 \cdot q_{100} \cdot q_{001}},$$

$$\cos(\gamma^*) = \frac{(q_{110}{}^2 - q_{100}{}^2 - q_{010}{}^2)}{2 \cdot q_{100} \cdot q_{010}}$$

2) **Step 2: We conduct modeling of three possible molecular structures of SIL.**

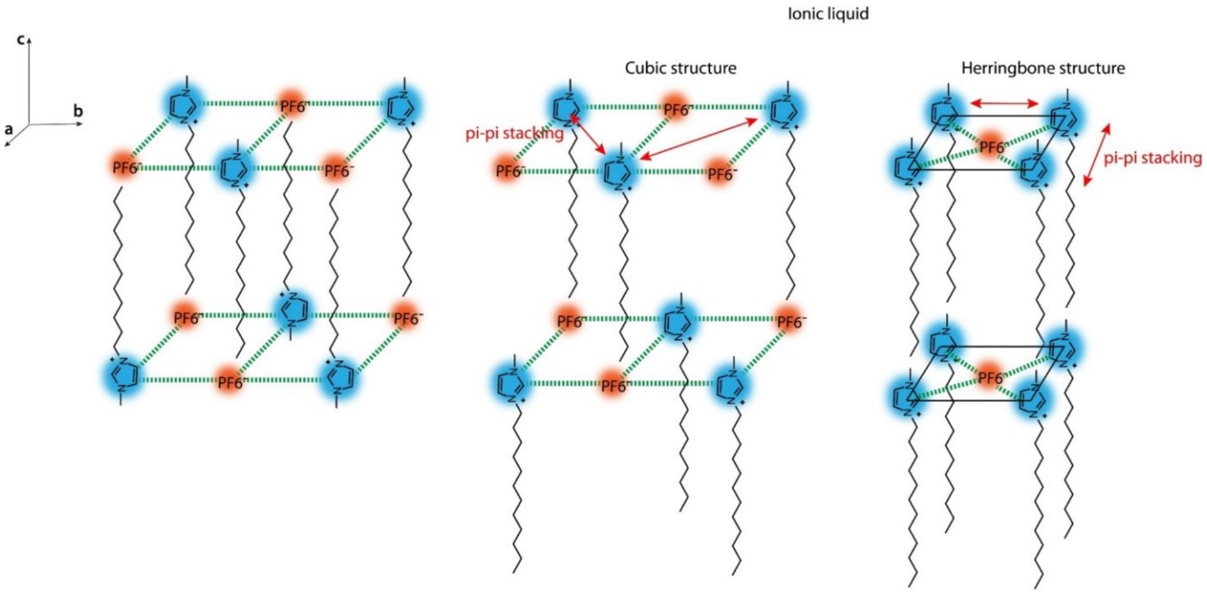

3) **Step 3: From the relations, we compare the parameters from modeling with the experimental result from GIWAXS measurement as bellow:**

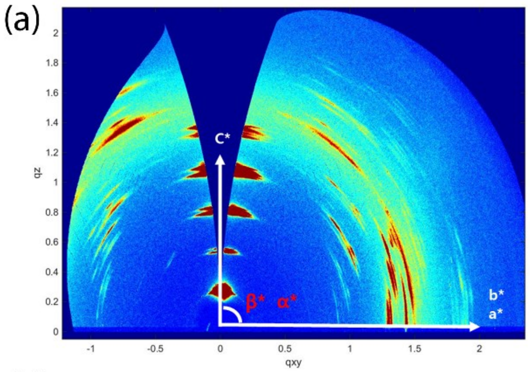

Experimental results

q_z (Å^{-1})	q_{xy} (Å^{-1})	Peak Indexing
0.270	0	(001)
0	1.2624	(-120)
0	1.4062	(110)
0	1.4267	(020)
0	1.608	(-210)
0	1.680	(-220)
0	1.824	(200)
0	2.03	(120)
0	2.26	(210)

(b) Base-centered monoclinic structure

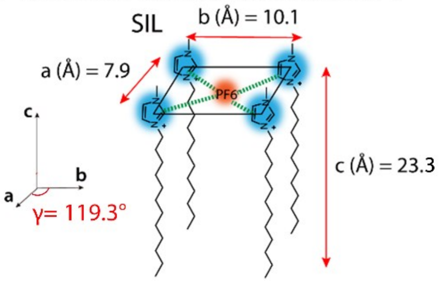

Parameters	SIL
a(Å)	7.90
b(Å)	10.10
c(Å)	23.27
γ(deg.)	119.30
Unit cell volume	1631.40

Fig. S10. **(a)** Calculation of the diffraction parameters of the thin-film SIL at room temperature obtained from GIWAXS measurements. **(b)** Schematic illustration of the base-centered monoclinic structure of the unit cell of the SIL and the lattice parameters of a (Å) = 7.9, b (Å) = 10.1, c (Å) = 23.27, and γ (˚) = 119.3.

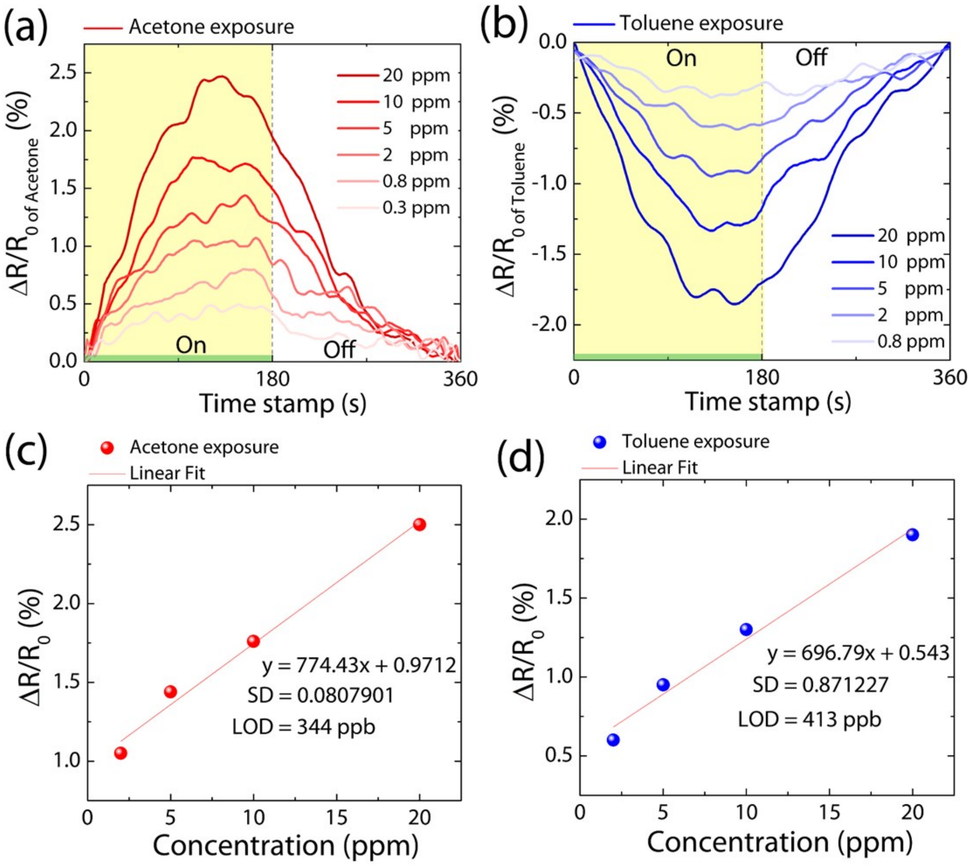

Fig. S11. Sub-ppm-level VOC detection in the TT:SIL TOCs. **(a)**, **(b)** The sensitivity of TT:SIL (1:7 w/w) and (1:3 w/w) TOCs upon acetone and toluene exposure, respectively, at low concentrations ranging from 20 ppm to 300 ppb. The limits of detection (LODs) of TT:SIL TOCs for **(c)** acetone and **(d)** toluene were calculated to be 344 ppb and 413 ppb, respectively, using the Inter-national Conference on Harmonization (ICH) model, in which the LOD is defined as 3.3 × (standard deviation/slope of regression line).

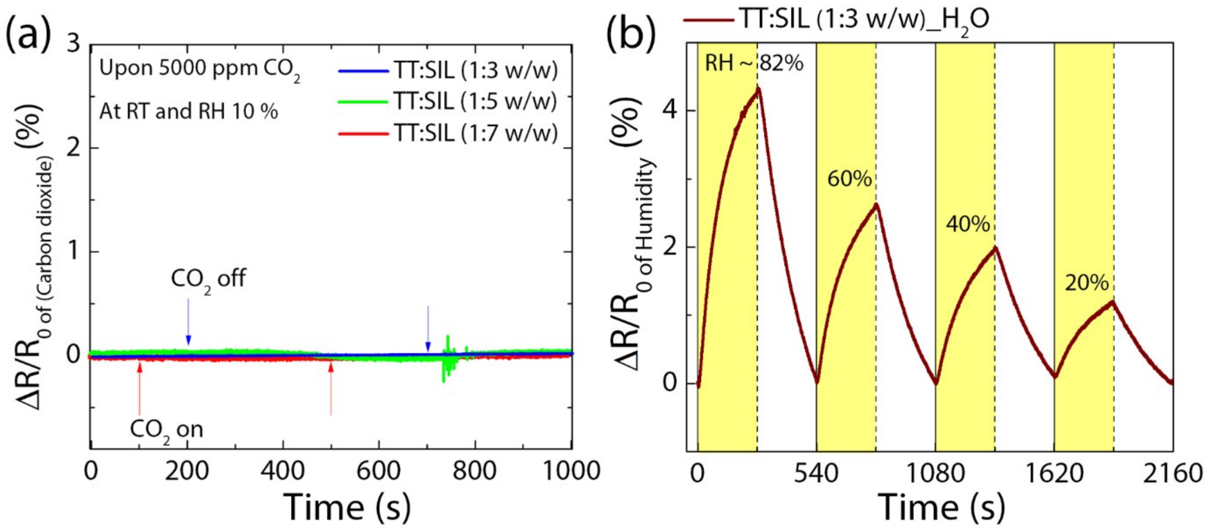

Fig. S12. **(a)** Characterization of the sensing property of the TT:SIL films with various blend ratios for carbon dioxide (CO_2). The red and blue arrows indicate the time of exposure (5000 ppm) and closure of the CO_2 gas valve, respectively, which indicates that the excess CO_2 gas does not influence the electrical properties of the TT:SIL TOCs. **(b)** Plot of the normalized resistance response of the TT:SIL TOCs for 300-sec pulses upon exposure to H_2O at various relative humidity value.

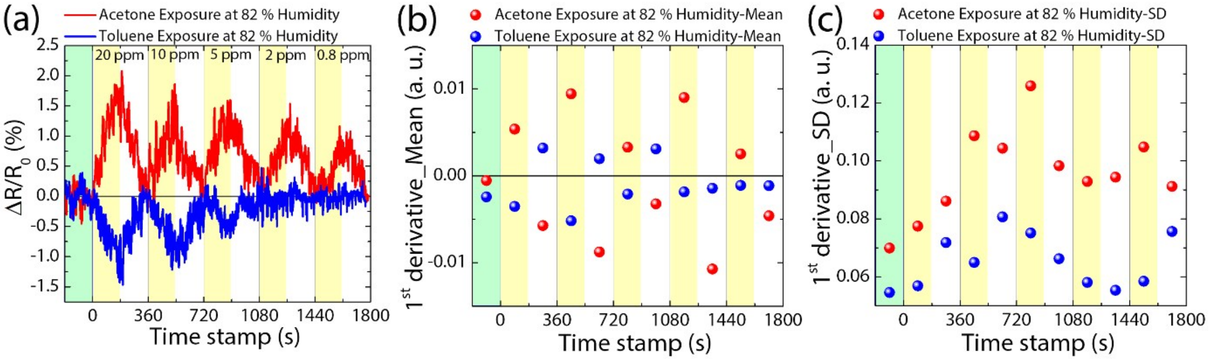

Fig. S13. (a) The electrical response of the TT:SIL TOCs upon acetone and toluene exposure at concentrations ranging from 20 ppm to 800 ppb under 82% humidity conditions. **(b), (c),** The mean and standard deviation (SD) of the primary derivative value of the obtained electrical response for 180-sec intervals, respectively. The light-yellow and cyan regions indicate the periods of exposure to the VOC and RH ~ 82%, respectively.

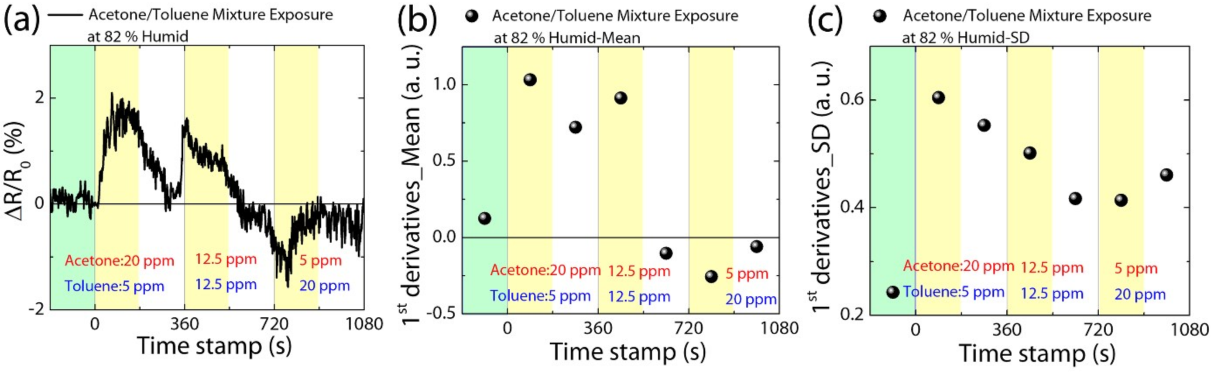

Fig. S14. Comparison of the electrical response to a mixture of acetone and toluene at high-humidity condition of RH ~ 82%. The light-yellow and cyan regions indicate the periods of exposure to the VOC and RH ~ 82%, respectively. **(b), (c),** The mean and standard deviation (SD) of the primary derivative value of the obtained electrical response for 180-sec intervals, respectively. The light-yellow and cyan regions indicate the periods of exposure to the VOC and RH ~ 82%, respectively.

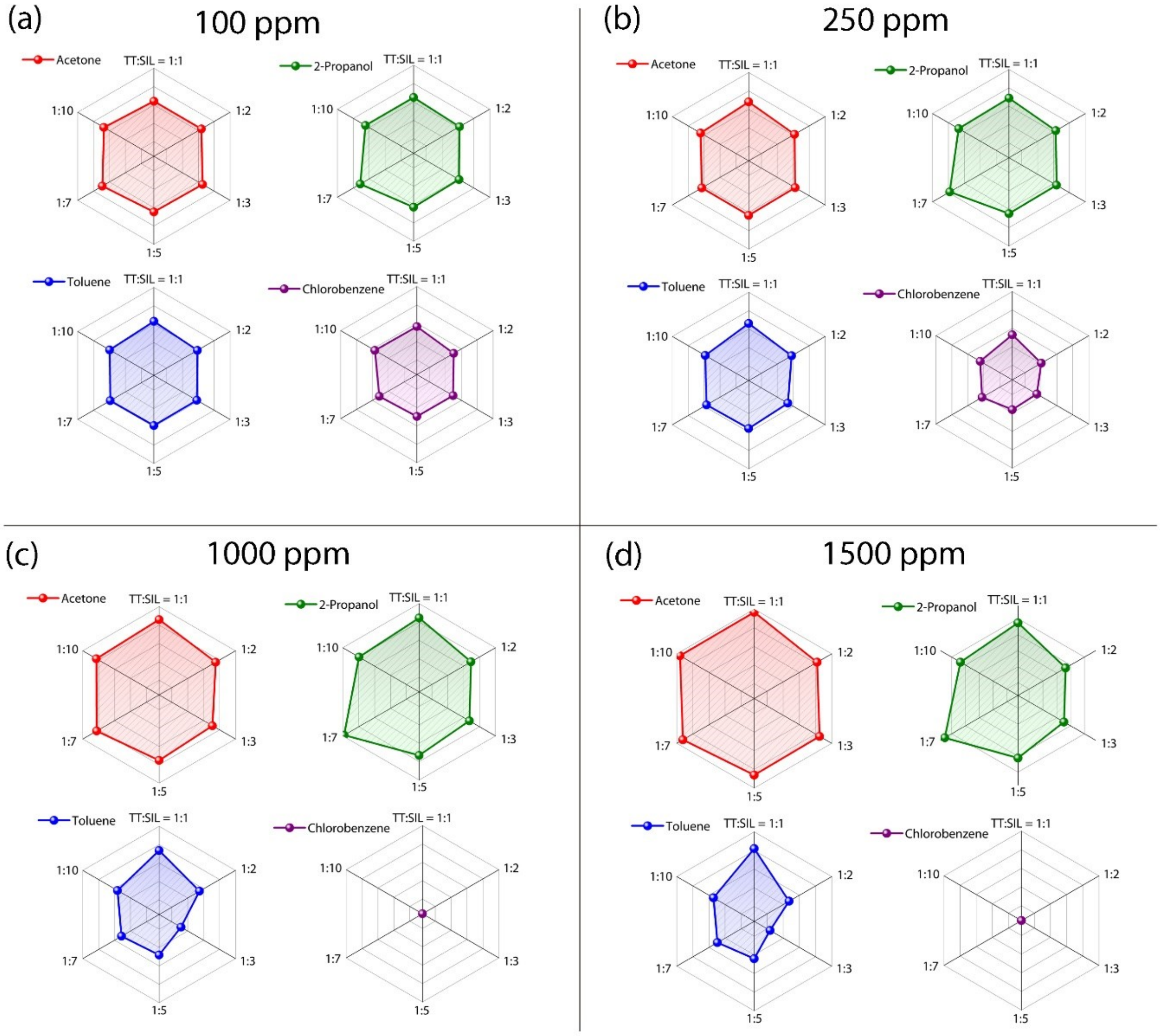

Fig. S15. Radar plot showing maximum electrical response of TT:SIL TOCs upon 4 different VOCs exposure at each blend ratio for (a) 100 ppm, (b) 250 ppm, (c) 1000 ppm and (d) 1500 ppm.